Electronic Supplementary Information

Highly Efficient Unidirectional Forward Scattering Induced by Resonant Interference in Metal-Dielectric Heterodimer

Song Sun,[1,2,] Dacheng Wang,[1,2] Zheng Feng,[1,2] and Wei Tan[1,2,*]*

[1]*Microsystem & Terahertz Research Center, China Academy of Engineering Physics, Chengdu, China 610200.*

[2]*Insititute of Electronic Engineering, China Academy of Engineering Physics, Mianyang, China 621999.*

*Corresponding author Emails: sunsong@mtrc.ac.cn, tanwei@mtrc.ac.cn

1. Additional formulation for $E||$dimer polarization

1.1. Explicit expressions of e-e, m-m and e-m interactions

The explicit expressions for electric-electric dipole interaction (e-e), magnetic-magnetic dipole interactions (m-m) and electric-magnetic dipole interactions (e-m) of metal-dielectric heterodimer can be represented as:

$$\sigma_{e-e}=\frac{\alpha_{1e}+\alpha_{2e}+2g_{yy}k^2\alpha_{1e}\alpha_{2e}}{1-{g_{yy}}^2k^4\alpha_{1e}\alpha_{2e}}\quad,\qquad \sigma_{m-m}=\frac{\alpha_{1m}+\alpha_{2m}-2g_{xx}k^2\alpha_{1m}\alpha_{2m}}{1-{g_{xx}}^2k^4\alpha_{1m}\alpha_{2m}}$$

$$\sigma_{e-m}=\frac{{g_{zx}}^2k^4\left(-{\alpha_{1m}}^2\alpha_{2e}+k^2\alpha_{1m}\left(2{g_{xx}}^2k^2\alpha_{1e}\alpha_{1m}+{g_{zx}}^2k^2\alpha_{1e}\alpha_{1m}+2g_{xx}\left(-\alpha_{1e}+\alpha_{1m}\right)\right)\alpha_{2e}\alpha_{2m}\right)}{\left(-1+{g_{xx}}^2k^4\alpha_{1m}\alpha_{2m}\right)\left(1+k^4\left(\left(-{g_{xx}}^2\alpha_{1e}-{g_{zx}}^2\alpha_{1m}\right)\alpha_{2e}+\left(-{g_{zx}}^2\alpha_{1e}-{g_{xx}}^2\alpha_{1m}+\left({g_{xx}}^2+{g_{zx}}^2\right)^2k^4\alpha_{1e}\alpha_{1m}\right.\right.\right.}$$
$$+\frac{\left.\left.\left.-{g_{zx}}^2k^4\left(\alpha_{1e}\left(-1+g_{xx}k^2\alpha_{1m}\right)^2+k^4\alpha_{1m}\left(\left(-2{g_{xx}}^2-{g_{zx}}^2\right)\alpha_{1e}+g_{xx}\left(g_{xx}+2\left({g_{xx}}^2+{g_{zx}}^2\right)k^2\alpha_{1e}\right)\alpha_{1m}\right)\alpha_{2e}\right)\alpha\right.\right.}{\left(-1+{g_{xx}}^2k^4\alpha_{1m}\alpha_{2m}\right)\left(1+k^4\left(\left(-{g_{xx}}^2\alpha_{1e}-{g_{zx}}^2\alpha_{1m}\right)\alpha_{2e}+\left(-{g_{zx}}^2\alpha_{1e}-{g_{xx}}^2\alpha_{1m}+\left({g_{xx}}^2+{g_{zx}}^2\right)^2k^4\alpha_{1e}\alpha_{1m}\alpha_{2e}\right.\right.\right.} \quad \text{(S1)}$$

Clearly, σ_{e-e} and σ_{m-m} are only related to the electric and magnetic polarizabilities of the two constituents of dimer, respectively, whereas σ_{e-m} involves complex interaction between electric and magnetic dipoles.

1.2. Scattered Far field calculation of metal-dielectric heterodimer

The scattered electric far field of heterodimer can be represented as the superposition of contributions from various dipole moments of each individual constituent.

$$E_{far}^{dimer}=\sum_{j=1,2}E_{far}^{P}+E_{far}^{m} \quad \text{(S2)}$$

where $E_{far}^{P}=\frac{k^2}{4\pi\varepsilon_0}(n\times P)\times n\frac{e^{ikr}}{r}$ and $E_{far}^{m}=-\frac{Zk^2}{4\pi}(n\times m)\frac{e^{ikr}}{r}$ are the electric far fields from electric dipole moment ***P*** and magnetic dipole moment ***m***, respectively. ***P*** and ***m*** are the solutions of Eq. (1) in the main text. ***n*** is the unit vector in the direction of observation point and *r* takes into account the spatial distance between the two nanoparticles.

2. Benchmark of analytical dipole-dipole model with full wave simulation

Fig. S1 compares the results of total extinction spectra and far field angular radiation patterns obtained by the analytical dipole-dipole interaction model and full wave simulation, for ***E***||dimer

and $\boldsymbol{E}\perp$dimer respectively. The two methods agree well with each other. The discrepancy is attributed to the volumetric charge distributions of the nanoparticle and the near field interaction between them. However, the full wave simulation cannot give the separate contributions (both amplitudes and phases) of ED_{dimer} and MD_{dimer}, therefore it cannot predict the optimal wavelength of Kerker condition for the heterodimer configuration.

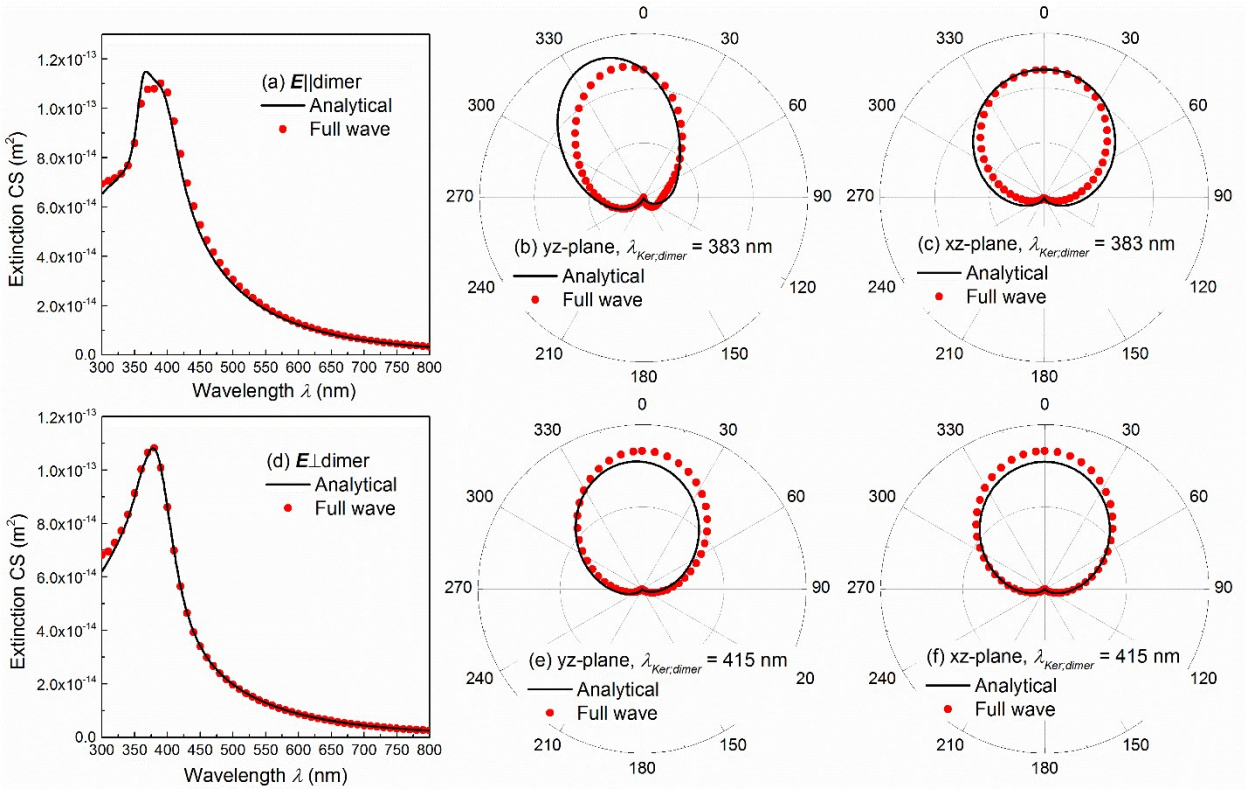

FIG. S1. Comparison between analytical dipole-dipole interaction model with full wave simulation, they two agree well with each other.

3. Effect of dielectric/metal nanoparticle size

For a metal-dielectric heterodimer, since its MD_{dimer} mainly comes from the dielectric constituent, the sizes of metal and dielectric nanoparticle as well as the gap distance are

cooperatively tuned so as to give an enhanced ED_{dimer} which up-matches the MD_{dimer} in phase (e.g. have equal real and imaginary parts) at a wavelength close to the resonance peak of dimer. This is where the optimal condition is achieved.

Figs. S2(a)-(c) show the real and imaginary parts of ED_{dimer} and MD_{dimer} for TiO_2 nanoparticle diameter D_d = 125 nm, 145 nm and 165 nm, respectively. The Ag nanoparticle diameter and dimer gap distance are kept at D_m = 55 nm and D_{gap} = 10 nm. Clearly, when D_d is smaller than the optimal value (= 145 nm), the intersection point of real parts of ED_{dimer} and MD_{dimer} occurs at a different wavelength compared to that of imaginary parts, which creates a mismatch and results in a low F/B ratio. On the other hand, when D_d is larger than the optimal value (= 145 nm), the real parts of ED_{dimer} and MD_{dimer} are completely separated, which also creates a mismatch and reduces the F/B ratio.

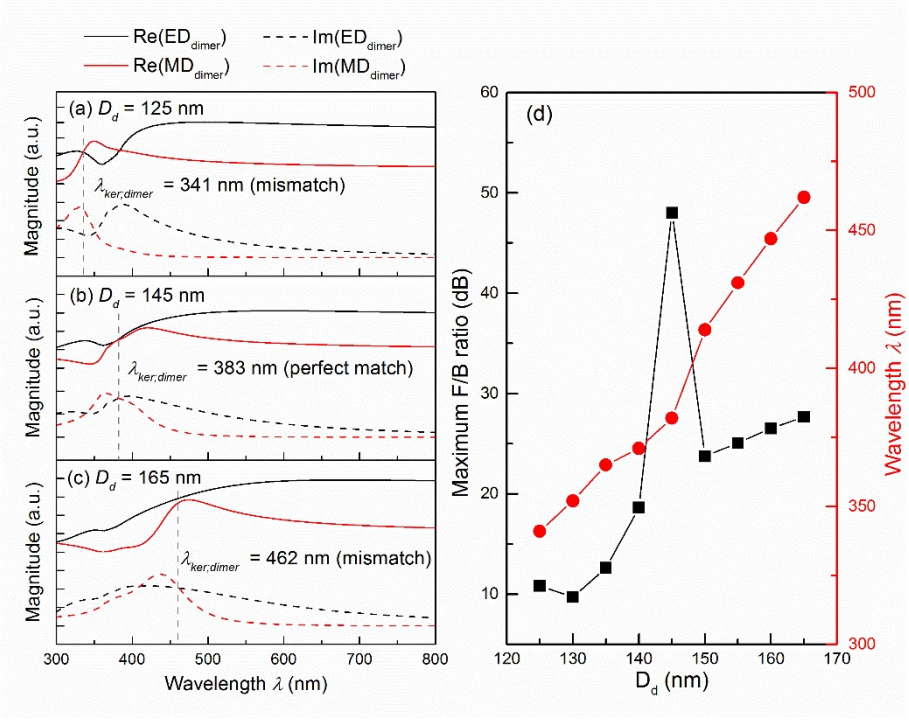

FIG. S2. (a)-(c) Real and imaginary parts of ED_{dimer} and MD_{dimer} with TiO_2 nanoparticle diameter D_d = 125 nm, 145 nm and 165 nm, respectively. (d) Effect of D_d on maximum achievable F/B ratios and associated operation wavelength.

Mismatch between ED_{dimer} and MD_{dimer} occurs when D_d moves away from the optimal value (= 145 nm). The Ag nanoparticle diameter and gap distance are fixed at D_m = 55 nm and D_{gap} = 10 nm, respectively.

Similarly, Figs. S3(a)-(c) show the real and imaginary part of ED_{dimer} and MD_{dimer} for Ag nanoparticle diameter D_m = 40 nm, 55 nm and 75 nm, respectively. The TiO_2 nanoparticle diameter and gap distance are kept at D_d = 145 nm and D_{gap} = 10 nm, respectively. Again, when D_m is smaller than the optimal value (= 55 nm), the real parts of ED_{dimer} and MD_{dimer} become separated, which reduces the maximum achievable F/B ratio. On the other hand, when D_m is larger than the optimal value (= 55 nm), the intersection point of real parts of ED_{dimer} and MD_{dimer} appears at a different wavelength compared to that of imaginary parts, which leads to a mismatch and results in a low F/B ratio.

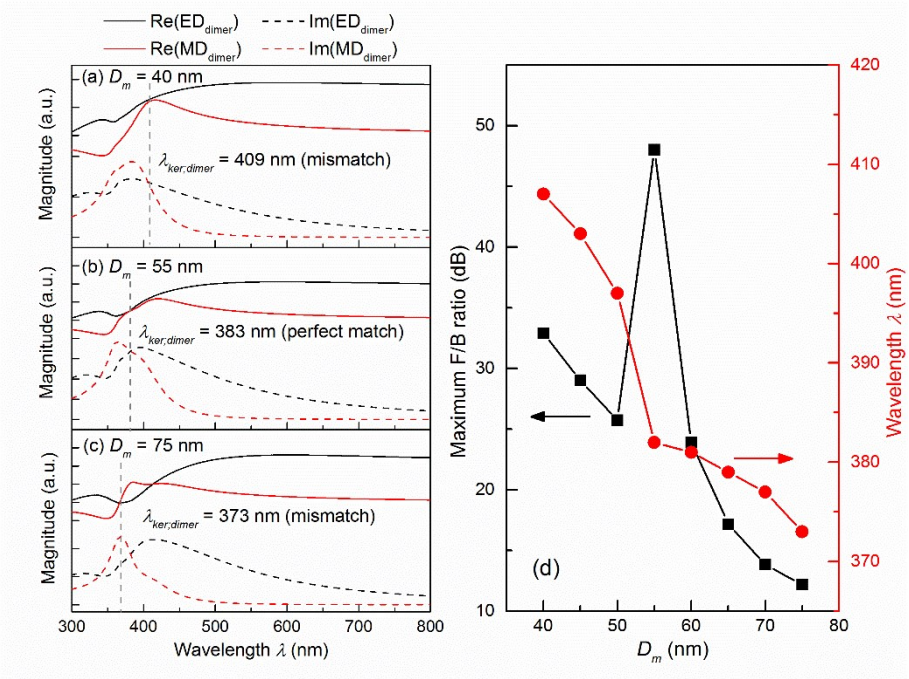

FIG. S3. (a)-(c) Real and imaginary parts of ED_{dimer} and MD_{dimer} with Ag nanoparticle diameter D_m = 40 nm, 55 nm and 75 nm, respectively. (d) Effect of D_m on maximum achievable F/B ratios and associated operation wavelength. Mismatch between ED_{dimer} and MD_{dimer} occurs when D_m moves away from the optimal value (= 55 nm). The TiO_2 nanoparticle diameter and gap distance are fixed at D_d = 145 nm and D_{gap} = 10 nm, respectively.

4. Efficient unidirectional forward scattering with a larger gap distance

Fig. S4(a) shows the total extinction spectra as well as the separated contributions of electric and magnetic dipolar response (ED_{dimer} and MD_{dimer}) for a heterodimer, which consists of a 54 nm diameter Ag nanoparticle and a 143 nm diameter TiO_2 nanoparticle with an intermediate 20 nm gap distance. ED_{dimer} and MD_{dimer} have equal magnitudes in the extinction spectrum at $\lambda_{Ker;dimer} = 385\ nm$, which is close to the resonance peak of dimer. Fig. S4(b) shows the real and imaginary parts of ED_{dimer} and MD_{dimer}, which proves that they are equal in both amplitudes and phases at $\lambda_{Ker;dimer} = 385\ nm$. Therefore, the first Kerker condition is satisfied and gives a maximum F/B ratio ≈ 45 dB, demonstrating an efficient unidirectional forward scattering pattern as shown in Fig. S4(c). It is proved that by corporately tuning the sizes of both metal and dielectric nanoparticles as well as the gap distance, fulfillment of the first Kerker condition at a wavelength close to the resonance peak can be achieved at a relatively large gap distance.

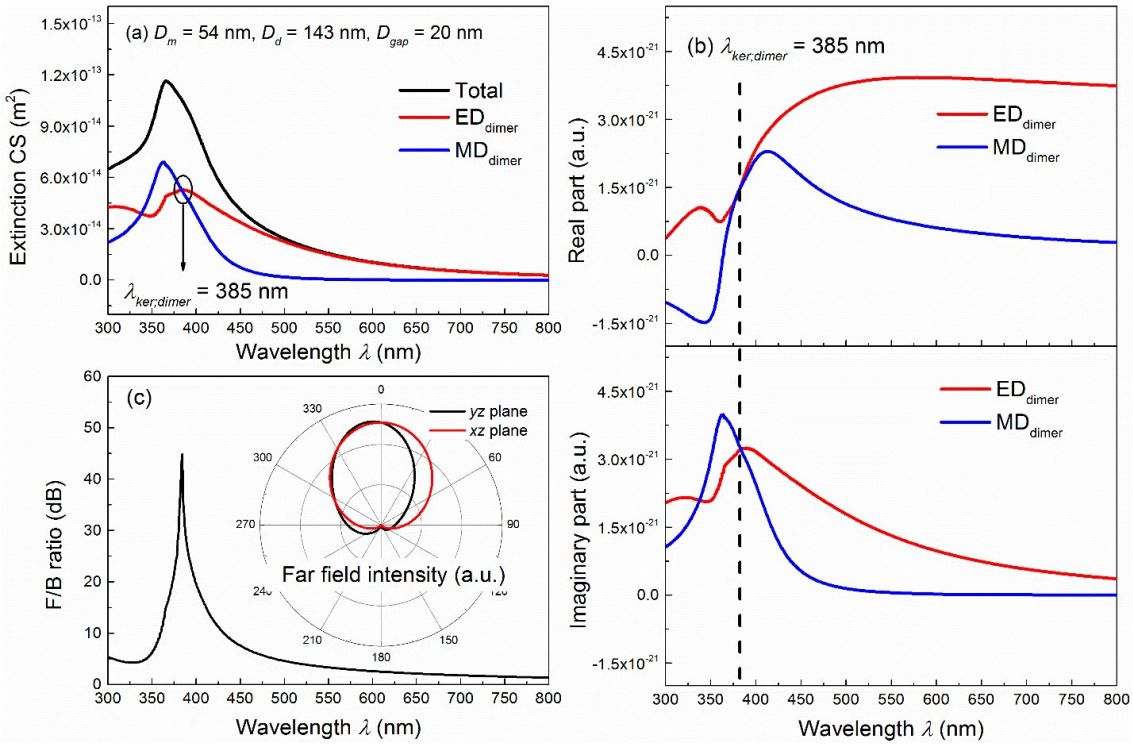

FIG. S4. Efficient unidirectional forward scattering for Ag-TiO_2 heterodimer with D_m = 54 nm, D_d = 143 nm and D_{gap} = 20 nm. (a) Extinction cross section. (b) Real and imaginary parts of ED_{dimer} and MD_{dimer}. (c) F/B ratio and field angular radiation pattern.

5. Weak coupling between metal and dielectric for $\boldsymbol{E}\perp$dimer polarization

For an incident plane wave propagates along the *z*-axis with electric field polarized along the *x*-axis (see Fig. S5(a)), which is perpendicular to the dimer axis ($\boldsymbol{E}\perp$dimer), the coupled electric and magnetic dipole moments in the dimer can be expressed as:

$$\begin{cases} m_{1y} = -\dfrac{\alpha_{1m}}{Z}E_0 + \alpha_{1m}k^2 g_{yy} m_{2y} \\ m_{2y} = -\dfrac{\alpha_{2m}}{Z}E_0 + \alpha_{2m}k^2 g_{yy} m_{1y} \\ m_{1z} = -i\dfrac{\alpha_{1m}\ k^2}{Z\ \varepsilon_0\varepsilon_r} g_{zx} P_{2x} - \alpha_{1m}k^2 g_{xx} m_{2z} \\ m_{2z} = i\dfrac{\alpha_{2m}\ k^2}{Z\ \varepsilon_0\varepsilon_r} g_{zx} P_{1x} - \alpha_{2m}k^2 g_{xx} m_{1z} \\ P_{1x} = \varepsilon_0\varepsilon_r\alpha_{1e}E_0 - \alpha_{1e}k^2 g_{xx} P_{2x} - i\varepsilon_0\varepsilon_r\alpha_{1e}Zk^2 g_{zx} m_{2z} \\ P_{2x} = \varepsilon_0\varepsilon_r\alpha_{2e}E_0 - \alpha_{2e}k^2 g_{xx} P_{1x} - i\varepsilon_0\varepsilon_r\alpha_{2e}Zk^2 g_{zx} m_{1z} \end{cases} \quad (S3)$$

and the total extinction CS can be written as:

$$\sigma_{ext} = \frac{4\pi}{kE_0} Im\left\{\frac{k^2}{4\pi\varepsilon_0\varepsilon_r}(P_{1x} + P_{2x}) - \frac{Zk^2}{4\pi}(m_{1y} + m_{2y})\right\} = \frac{k}{E_0} Im\{ED_{dimer} + MD_{dimer}\} \quad (S4)$$

Rearranging the solution of Eq. (S4), we could obtain the separated electric-electric (e-e), magnetic-magnetic (m-m) and electric-magnetic (e-m) as:

$$\sigma_{e-e} = \frac{\alpha_{1e} + \alpha_{2e} - 2g_{xx}k^2\alpha_{1e}\alpha_{2e}}{1 - {g_{xx}}^2 k^4 \alpha_{1e}\alpha_{2e}}, \qquad \sigma_{m-m} = \frac{\alpha_{1m} + \alpha_{2m} + 2g_{yy}k^2\alpha_{1m}\alpha_{2m}}{1 - {g_{yy}}^2 k^4 \alpha_{1m}\alpha_{2m}}$$

$$\sigma_{e-m} = \frac{{g_{zx}}^2 k^4 \left(-{\alpha_{1e}}^2(-1 + g_{xx}k^2\alpha_{2e})^2\alpha_{1m} + \alpha_{1m}\alpha_{2e}(-1 + g_{xx}k^2\alpha_{1e})^2\alpha_{2e}\right)}{\left(-1 + {g_{xx}}^2 k^4\alpha_{1e}\alpha_{2e}\right)\left({g_{xx}}^4 k^8 \alpha_{1e}\alpha_{1m}\alpha_{2e}\alpha_{2m} - (1 + {g_{zx}}^2 k^4\alpha_{1m}\alpha_{2e})(-1 + {g_{zx}}^2 k^4\alpha_{1e}\alpha_{2m}) - {g_{xx}}^2 k^4 \right.} + \frac{{g_{zx}}^4 k^8 \alpha_{1e}\alpha_{2e}\alpha_{1m}\alpha_{2m}(-\alpha_{2e} + \alpha_{1e}(-1 + 2g_{xx}k^2\alpha_{2e}))}{\left(-1 + {g_{xx}}^2 k^4\alpha_{1e}\alpha_{2e}\right)\left({g_{xx}}^4 k^8 \alpha_{1e}\alpha_{1m}\alpha_{2e}\alpha_{2m} - (1 + {g_{zx}}^2 k^4\alpha_{1m}\alpha_{2e})(-1 + {g_{zx}}^2 k^4\alpha_{1e}\alpha_{2m}) - {g_{xx}}^2 k^4 (\alpha \right.} \quad (S5)$$

For $\boldsymbol{E}\perp$dimer polarization, the multipolar Mie resonances of the single Ag and TiO_2 nanoparticles are given in Figs. S5(b) and S5(c) respectively, which are identical to those in Fig. 1 in the main text. Fig. S5(d) shows the total extinction CS of dimer as well as the associated electric and magnetic dipolar responses ED_{dimer} and MD_{dimer}. It is found that for $\boldsymbol{E}\perp$dimer polarization, MD_{dimer} is almost identical to that of pure TiO_2, while ED_{dimer} is only slightly enhanced and blue-shifted to that of pure Ag. As a result, the first Kerker condition of dimer is achieved at the same wavelength as that of pure TiO_2, e.g. $\lambda_{Ker;dimer} = \lambda_{Ker;TiO2} = 415\ nm$. This is

essentially due to the weak coupling between metal and dielectric constituents as shown in Fig. S5(e). The e-e interaction is weak under $\boldsymbol{E}\perp$dimer excitation since parallel electric dipole moments are excited in metal and dielectric nanoparticles. While the m-m interaction is still solely due to the TiO_2, the e-m interaction is too weak to induce any pronounced effect on the overall MD_{dimer}. The weak coupling is clearly visualized in the electric and magnetic near field distributions in Fig. S5(f). Compared to $\boldsymbol{E}$||dimer polarization, no electric field enhancement is observed in the gap region, and the magnetic field enhancement is solely concentrated inside the dielectric nanoparticle and has negligible effect on the adjacent metal nanoparticle. Therefore, for $\boldsymbol{E}\perp$dimer polarization, the scattering property of dimer behaves similarly as that of pure TiO_2 nanoparticle at $\lambda_{Ker;dimer} = \lambda_{Ker;TiO2} = 415\ nm$, where both the real and imaginary parts of ED_{dimer} and MD_{dimer} are equal as shown in Fig. S5(g). The resultant F/B ratio has a maximum value ≈ 33 dB, and its corresponding far field angular radiation pattern closely resembles that of pure TiO_2 nanoparticle as shown in Fig. S5(h).

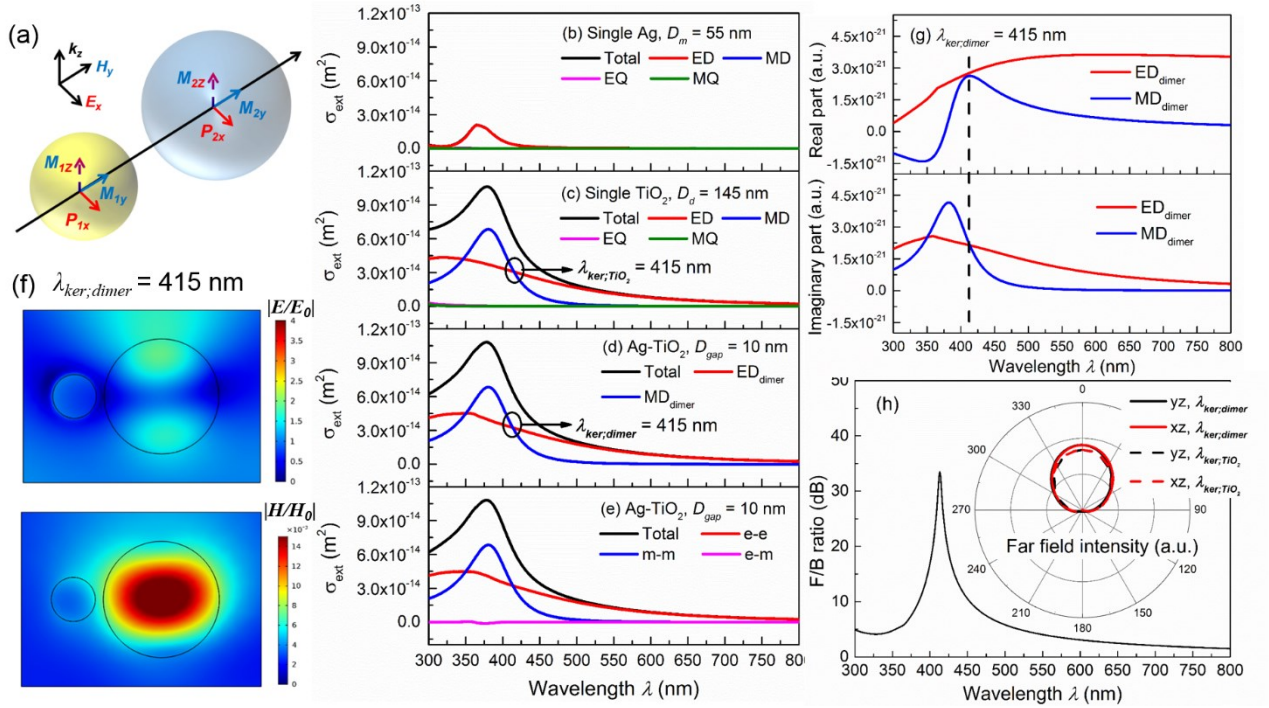

FIG. S5. First Kerker condition for $\boldsymbol{E}\perp$dimer situation, where the geometrical parameters are the same as those in Fig. 1 in the main text. (a) Schematic of dipole-dipole interaction model for $\boldsymbol{E}\perp$dimer. (b) and (c) Multipole Mie resonances of a single Ag nanoparticle and a single TiO_2 nanoparticle. (d) Overall electric and magnetic dipole response (ED_{dimer} and MD_{dimer}) of Ag-TiO_2 heterodimer. The first Kerker condition of dimer is equal to that of pure TiO_2 nanoparticle at $\lambda_{Ker;dimer} = \lambda_{Ker;TiO2} = 415\ nm$, due to the weak coupling for $\boldsymbol{E}\perp$dimer polarization. (e) Separated contributions from electric-electric interaction (e-e), magnetic-magnetic interaction (m-m), and electric-magnetic interaction (e-m). (f) Simulated electric and magnetic near field distribution of Ag-TiO_2 heterodimer at $\lambda_{Ker;dimer}$. (g) Real and imaginary parts of ED_{dimer} and MD_{dimer}. (h) Front-to-back ratio (F/B ratio) in dB. Inset: comparison of far field angular radiation patterns at *yz*- and *xz*-planes between heterodimer (solid line) and bare TiO_2 nanoparticle (dashed line) at their respective first Kerker conditions.

Since the weak coupling between metal and dielectric nanoparticles mainly results from the polarization of incidence ($\boldsymbol{E}\perp$dimer), changing the geometrical parameters of dimer structure will have limited effect on the optical response. We confirms this point by changing the gap distance D_{gap} over a broad range, and little change has been observed in the total extinction CS as shown in Fig. S6(a). The changes in real and imaginary parts of ED_{dimer} and MD_{dimer} are shown in Fig. S6(b), where MD_{dimer} remain identical regardless of D_{gap} due to the constant m-m contribution solely from TiO_2 and negligible e-m interaction. Nevertheless, it has a marginal effect on ED_{dimer} due to the weak e-e interaction, which creates a slight mismatch. The resultant maximum achievable F/B ratios and the associated wavelengths are shown in Fig. S6(c). The maximum F/B ratio occurs at a constant wavelength = 415 nm with a change in magnitude up to 20% with respect to the gap distance, which is fairly stable compared to that for $\boldsymbol{E}||$dimer case (see Fig. 3 in the main text).

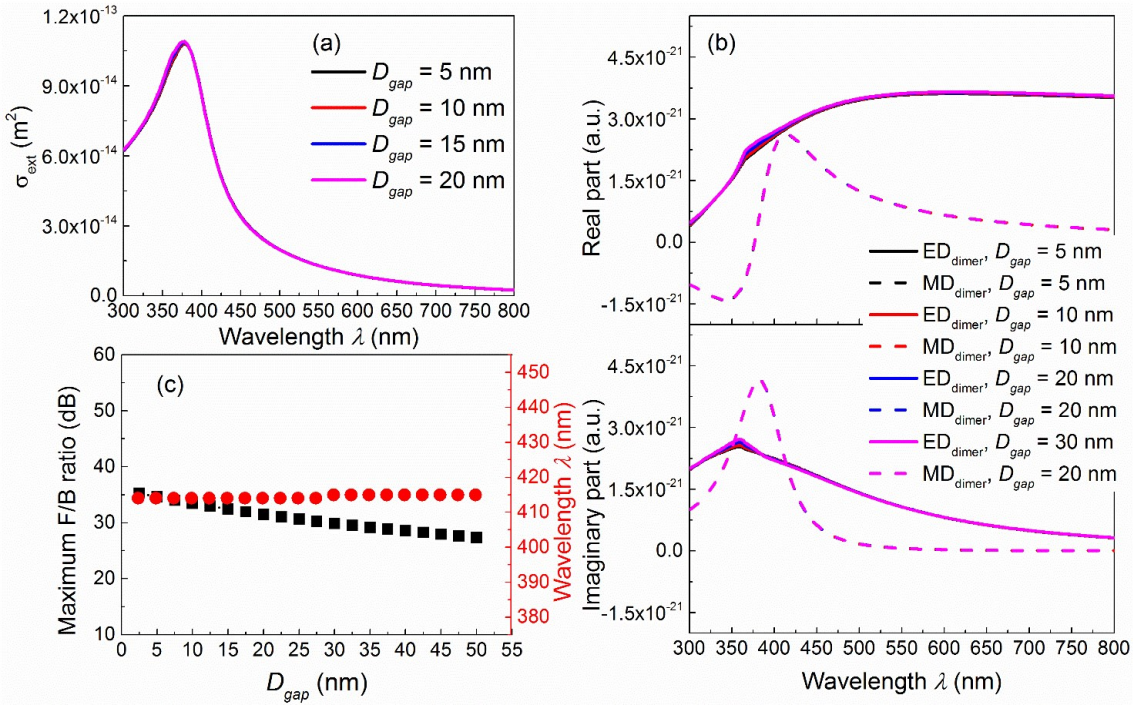

FIG. S6. Effect of gap distance D_{gap} on: (a) extinction spectra of heterodimer; (b) real and imaginary parts of electric and magnetic dipole moments ED_{dimer} and MD_{dimer}; and (c) maximum achievable F/B ratios and associated operation wavelength for $\boldsymbol{E}\perp$dimer polarization. Gap distance has limited effect on optical response of dimer due to intrinsic weak interaction between metal and dielectric nanoparticles.

6. First Kerker condition of optimized TiO_2-TiO_2 dielectric dimer

Figs. S7(a) and (b) show the multipole Mie resonances of single TiO_2 nanoparticle of D_d = 145 nm and D_d = 128 nm respectively. Both dielectric constituents have pronounced electric and magnetic resonances. Fig. S7(c) shows the overall ED_{dimer} and MD_{dimer} for the TiO_2-TiO_2 dimer with a gap distance D_{gap} = 39 nm. The coupling between these multipolar resonances yields an enhanced and red-shifted ED_{dimer} as well as an enhanced and blue-shifted MD_{dimer}, which gives the first Kerker condition at a wavelength $\lambda_{Ker;dimer} = 380\ nm$ that is far from the resonant peak. As

shown in Fig. S7(d), the enhanced ED_{dimer} is solely attributed to the e-e interaction, and the enhanced MD_{dimer} is due to the superposition of m-m and e-m interactions. Unlike Ag-TiO_2 heterodimer whose MD_{dimer} is relatively stable, the MD_{dimer} of TiO_2-TiO_2 dimer is significantly enhanced which intersects with ED_{dimer} at an off-resonance wavelength. Therefore, although a fairly good match between ED_{dimer} and MD_{dimer} can be obtained (Fig. S7(e)) to give a decent F/B ratio (Fig. S7(f)), the undesired off-resonance first Kerker condition is still inevitable with the pure dielectric dimer.

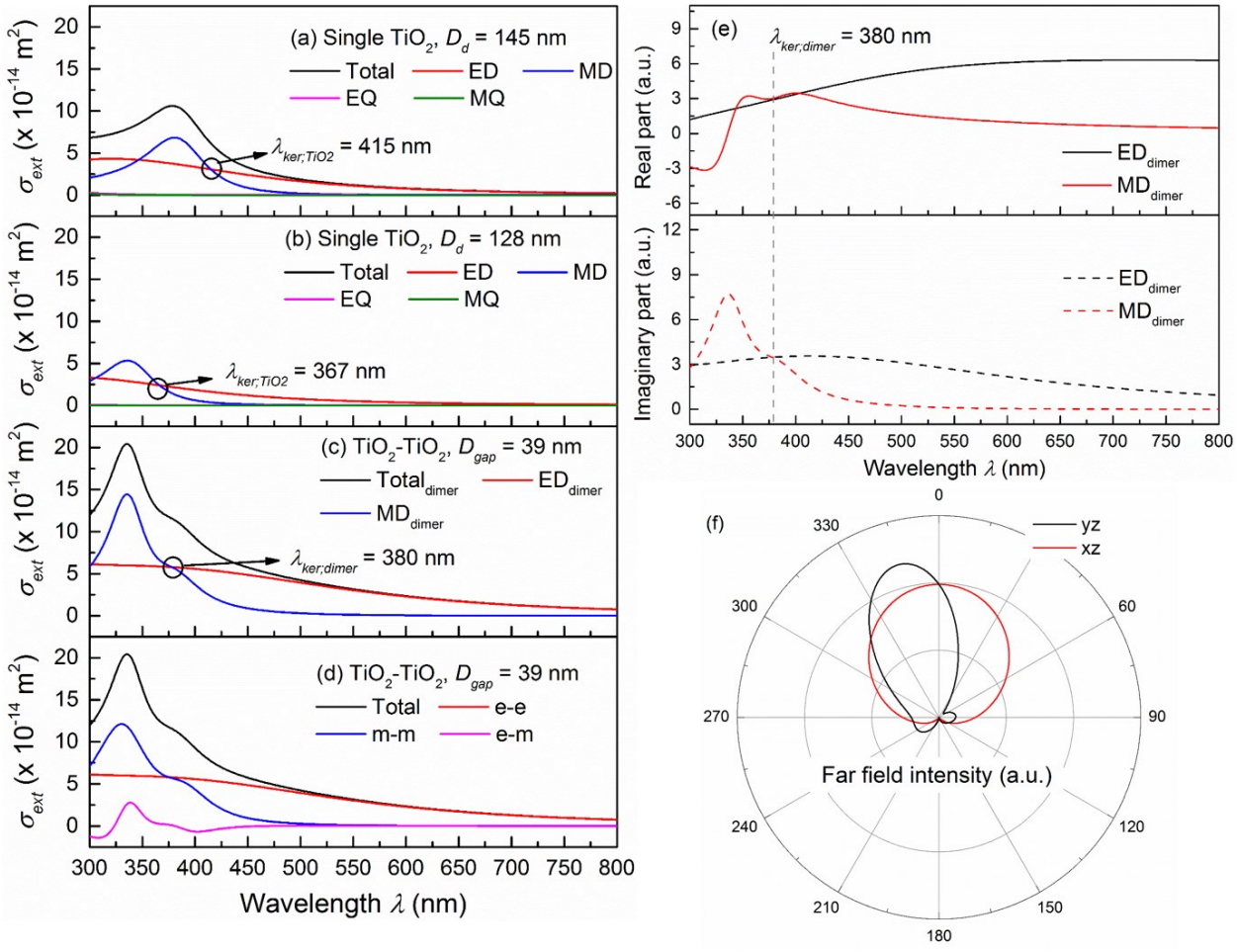

FIG. S7. Coupling of optimized TiO_2-TiO_2 dimer. (a) and (b) Multipole Mie resonances of 145 nm and 128 nm TiO_2 nanoparticle respectively. (c) Overall electric and magnetic dipole resonances ED_{dimer} and MD_{dimer} of TiO_2-TiO_2 dimer

with a gap distance D_{gap} = 39 nm. (d) Separated contributions of e-e, m-m and e-m interaction. (e) Real and imaginary parts of ED_{dimer} and MD_{dimer}. (f) Far field angular radiation patterns at $\lambda_{Ker;dimer} = 380\ nm$.

7. Additional data for Au-GaP dimer

Figs. S8(a) and S8(b) show the multipole Mie resonances of a single Au nanoparticle with diameter D_m = 80 nm and a single GaP nanoparticle with diameter D_d = 136 nm. The first Kerker condition for single GaP nanoparticle is satisfied at $\lambda_{Ker;GaP} = 540\ nm$. Fig. S8(c) shows the overall ED_{dimer} and MD_{dimer} of Au-GaP dimer with gap distance D_{gap} = 20 nm. The first Kerker condition of Au-GaP dimer is blue-shifted to $\lambda_{Ker;dimer} = 522\ nm$, which is much closer to the resonance peak compared to that of pure GaP nanoparticle. Fig. S8(d) illustrates the separated contribution of e-e, m-m and e-m interactions. Fig. S8(e) shows the real and imaginary parts of ED_{dimer} and MD_{dimer}, which are equal in both amplitudes and phases at $\lambda_{Ker;dimer} = 522\ nm$.

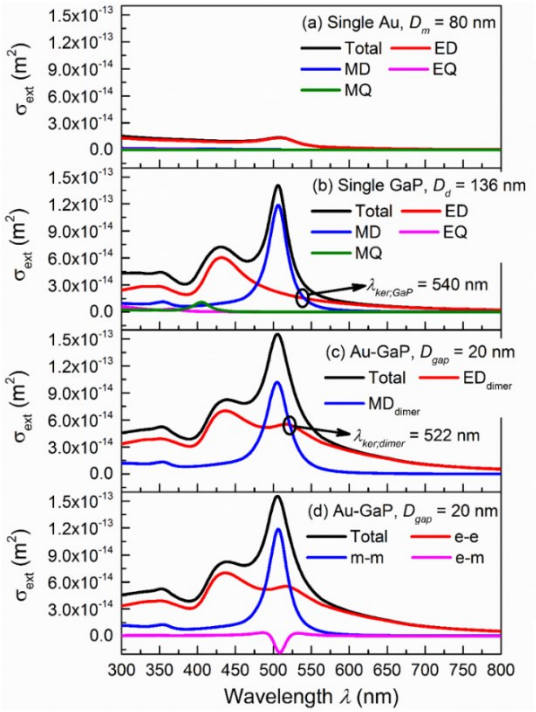

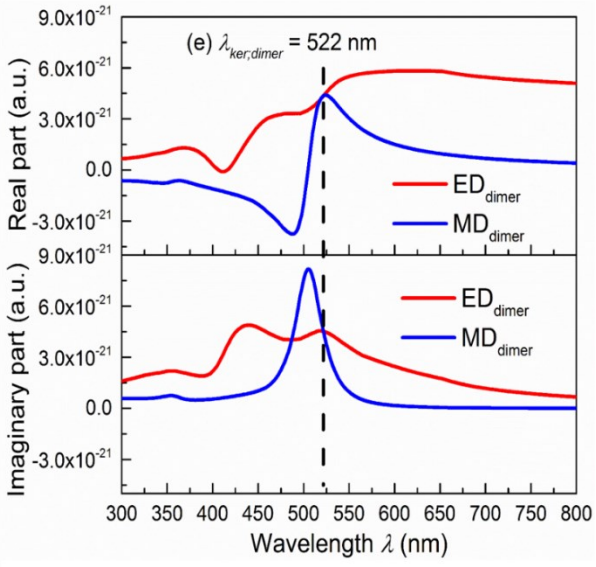

FIG. S8. First Kerker condition of Au-GaP dimer. (a) and (b) Multipole Mie resonances of single Au and GaP nanoparticle, respectively. (c) Overall electric and magnetic dipole resonances ED_{dimer} and MD_{dimer} of Au-GaP dimer. (d) Separated contributions of e-e, m-m and e-m interaction. (e) Real and imaginary parts of ED_{dimer} and MD_{dimer}.

8. Additional data for absorption, scattering and extinction cross-sections

Figs. S9(a)-(c) show the details of absorption, scattering and extinction cross-sections for Ag-TiO_2 dimer and its individual metal and dielectric constituents, while Figs. S9(d)-(f) show the corresponding results for Au-GaP dimer and its individual metal and dielectric constituents.

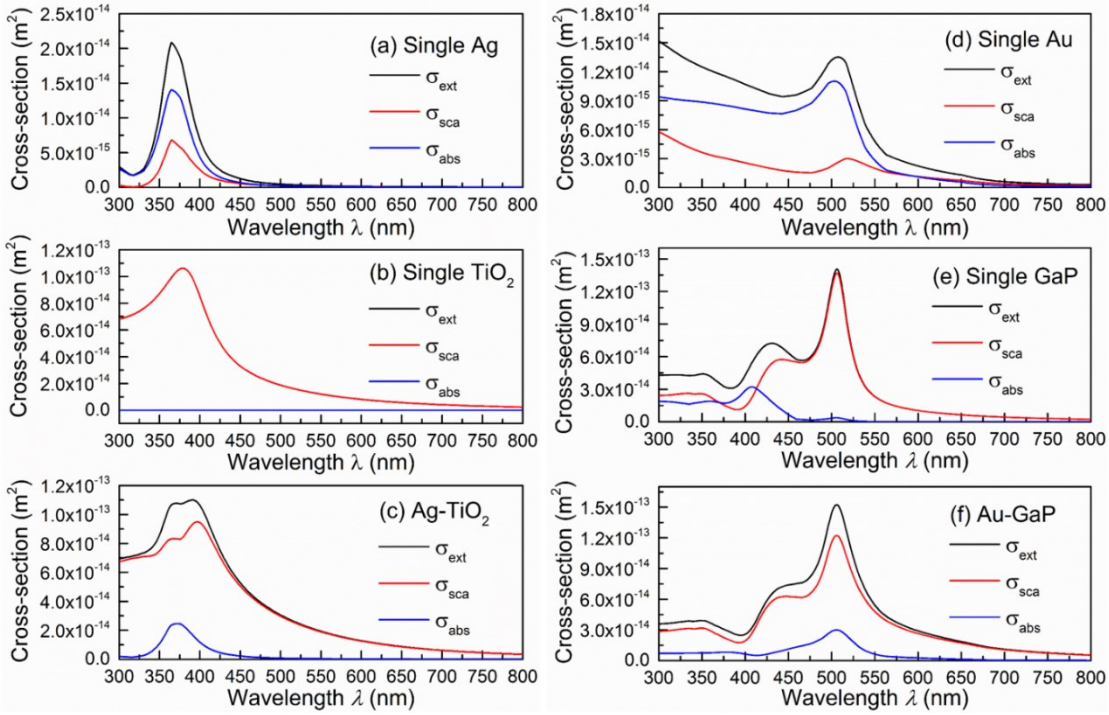

FIG. S9. Absorption (σ_{abs}), scattering (σ_{sca}) and extinction (σ_{ext}) cross-sections for: (a) a single Ag nanoparticle with diameter D_m = 55 nm; (b) a single TiO_2 nanoparticle with diameter D_d = 145 nm and (c) the Ag-TiO_2 dimer with gap distance D_{gap} = 10 nm. Similarly, (d) a single Au nanoparticle with diameter D_m = 80 nm; (e) a single GaP nanoparticle with diameter D_d = 136 nm and (f) the Au-GaP dimer with gap distance D_{gap} = 20 nm.

To better understand the suppression of absorption in the heterodimer, Fig. S10 compares absorption and scattering parts between Ag-TiO_2 dimer and its individual metal/dielectric constituent. The results show that for a pure Ag nanoparticle, the absorption σ_{abs} is larger than its scattering counterpart σ_{sca}, thus dominates the overall extinction $\frac{\sigma_{abs}}{\sigma_{ext}} = \frac{\sigma_{abs}}{\sigma_{sca} + \sigma_{abs}} \approx 70\%$. On the other hand, although σ_{abs} of Ag-TiO_2 dimer is 1.7 times that of a pure Ag nanoparticle, introducing a large lossless TiO_2 nanoparticle results in a much stronger σ_{sca} of heterodimer that is 15 times that of a pure Ag nanoparticle, thereby significantly suppressing the percentage of absorption in the total energy extinction $\frac{\sigma_{abs}}{\sigma_{ext}} = \frac{\sigma_{abs}}{\sigma_{sca} + \sigma_{sca}} \approx 20\%$.

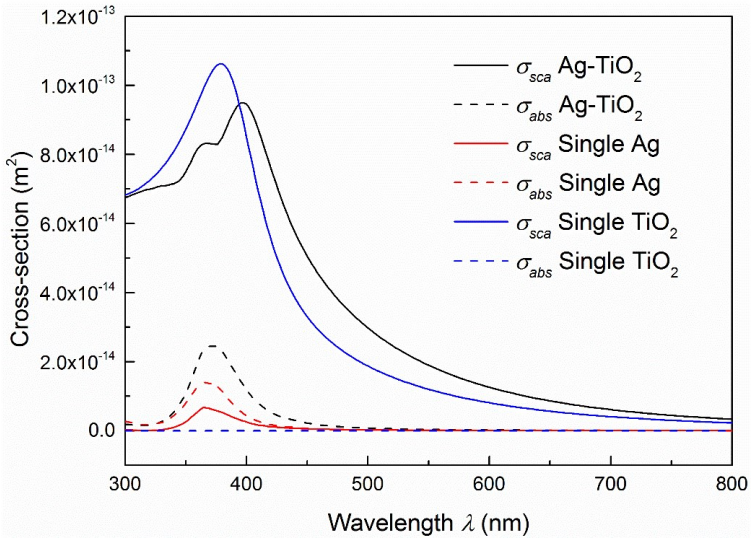

FIG. S10. Comparison of absorption and scattering parts between Ag-TiO_2 dimer and its individual metal/dielectric constituent.